Electric Propulsion Propellant Flow within Vacuum Chamber

IEPC-2015-360／ISTS-2015-b-360

Presented at Joint Conference of 30th International Symposium on Space Technology and Science
34th International Electric Propulsion Conference and 6th Nano-satellite Symposium,
Hyogo-Kobe, Japan
July 4 – 10, 2015

Yoshinori Nakayama[1] and Masahiro Nakamura[2]
National Defense Academy, Yokosuka, Kanagawa, 239-8686, Japan

Abstract: The thrusters are performed in vacuum chambers in the development and durability estimation; ground test. Since the propellant reflects on the chamber wall until the propellant is pumped out, the back pressure in the ground test operation is higher than that in space operation. The back pressure affects the plasma production, the neutralization, and the erosion by the charge-exchange ion. Accordingly, the performance and durability may be over/under-estimated. Through the numerical analysis, it becomes clear that the propellant distribution in the chamber is not uniform, and that the distribution is influenced by the number and location of the vacuum pumps, the chamber shape, and the thruster location.

Nomenclature

A	=	exit area [m^2]
C	=	conductance [m^3/s]
Ci	=	ion production cost [W/A]
D	=	diameter of vacuum chamber [m]
I	=	current [A]
L	=	length of vacuum chamber [m]
M	=	mass weight [kg/particle]
$\dot{m}$	=	mass flow rate [kg/s]
n	=	number density [particle/m^3]
$\dot{n}$	=	particle number flow rate [particle/s]
N	=	number of particle [particle]
nr	=	number of reflection [-]
p	=	pressure [Pa] or [mPa]
P	=	electric power
S	=	surface area [m^2], or thruster area [m^2]
t	=	time [s]
T	=	temperature [K]
v	=	velocity [m/s]
V	=	volume of vacuum chamber [m^3]
W	=	characteristic length [m]
L/D	=	aspect ratio of vacuum chamber [-]
A/S	=	aperture ratio of exit area to thruster area [-]

[1] Associate Professor, Department of Aerospace Engineering, ynakayam@nda.ac.jp.
[2] Graduate Student, Department of Aerospace Engineering, em53019@nda.ac.jp.

β = ratio of back pressure to discharge chamber pressure [-]
γ = ratio of downstream pressure to discharge chamber pressure [-]
η = propellant utilization efficiency [-]

Subscription:
dc = discharge chamber
dw = downstream
b = beam
CEX = charge-exchange
p = pump
r = resident
to = total
v = vacuum chamber
$'$ = in vacuum chamber operation
$\bar{}$ = average

I. Introduction

ELECTRIC propulsion achieve high specific impulse for long durations. Therefore, they are installed in many spacecraft as the main propulsion system and as an attitude control system. Development of more efficient electric propulsion might give birth to a wide variety of related applications.

In development and durability estimation of electric propulsion systems, vacuum chambers are necessary as their ground test facilities. Since the propellant particle reflects on the chamber wall, the pressure around electric propulsion system in case of ground-test operation is higher than that in case of in-space operation.[1-4] In addition, the propellant distribution within the vacuum chamber is not uniform. Therefore, it seems that the investigations of the pressure difference are significant for appropriate estimation of electric propulsion durability.

The objectives of this study are (1) to derive and discuss the influence of the vacuum chamber configuration to the back pressure, (2) to derive and discuss the influence of the back pressure to the thruster performance, (3) to evaluate and discuss the location of the vacuum pumps and the thruster, and (4) to discuss the prediction method for the estimation the thruster performance in space operation from that in the test facility operation.

II. Theoretical Analyses

In a vacuum chamber, the propellant particles emitted from an electric propulsion thruster are reflected on the surface of the chamber wall, and retained within the vacuum chamber until they are evacuated by the vacuum pumps. Therefore, the back pressure around the thruster in the vacuum chamber operation is higher than that in the space operation. The back pressure affects the thruster performance and its durability. In this section, at first, the expressions for the influence of the vacuum chamber configuration to the back pressure is derived and discussed. Subsequently, the expressions for the influence of the back pressure to the thruster performance is derived and discussed.

A. Vacuum Evacuation

The average travel time of a particle between successive impacts on the vacuum chamber wall is expressed in the following equation with the characteristic length of the chamber and the particle velocity.

$$\bar{t} = \frac{W}{\bar{v}} \tag{1}$$

The characteristic length of the chamber is almost equal to the cubic root of the vacuum chamber volume. The average reflection number of a particle is expressed in the following equation with the surface area of the vacuum chamber, the total area of the high vacuum pumps, and the evacuation efficiency of the pumps.

$$nr = \frac{S_v}{\eta_p S_p} \tag{2}$$

Substituting Eq. (2) for Eq. (1), the average resident time is derived.

$$\bar{t_r} = \bar{t} \times nr = \frac{W}{\bar{v}} \cdot \frac{S_v}{\eta_p S_p} \tag{3}$$

The total number of the average resident particles is obtained for the product of the number flow rate and the average resident time. Subsequently, the average particle number density is obtained the ratio of the total number of particles to the vacuum chamber volume.

$$\bar{n} = \frac{\overline{N_{to}}}{V} = \frac{\dot{n}}{V} \times \frac{W}{\bar{v}} \cdot \frac{S_v}{\eta_p S_p} = \frac{\dot{n}}{\bar{v}} \times W \times \frac{S_v}{V} \times \frac{1}{\eta_p S_p} \tag{4}$$

This equation indicates that the particle number density depends on the ratio of the surface area to the volume of the chamber. The configuration of the conventional vacuum chamber is cylindrical. The surface area and the volume are expressed in the following equations with the chamber diameter and the length.

$$V = \frac{\pi}{4} D^2 L \tag{5}$$

$$S_v = \pi D L + \frac{\pi}{2} D^2 \tag{6}$$

Eliminating of the chamber length from Eq. (6) with Eq. (5) leads the following equation.

$$S_v = \frac{4V}{D} + \frac{\pi}{2} D^2 \tag{7}$$

Differentiate Eq. (7) with respect to the chamber diameter leads the following equation.

$$\frac{dS_v}{dD} = -\frac{4V}{D^2} + \pi D \tag{8}$$

Derived from the Eq. (8), the length for the minimum surface area is derived.

$$D^3 = \frac{4}{\pi} V \tag{9}$$

$$D = L = \sqrt[3]{\frac{4}{\pi} V} \tag{10}$$

These equations express that the ratio of the surface area to the volume is minimum when the diameter is equal to the length of the vacuum chamber. The back pressure is proportional to the average particle number density, as expressed in the following equation.

$$p_b = \bar{n} k T \tag{11}$$

Accordingly, it becomes clear that the back pressure is minimum when the aspect ratio of the vacuum chamber is unity.

B. Influence of Back Pressure to Thruster Performance

In this section, the influence of back pressure to gridded ion thruster performance is discussed. This discussion and technical expertise may have applicability to the discussion on the other electric propulsion thrusters: hall-effect ion thruster, arcjet thruster, and so on.

Figure 1 depicts the schematic of the propellant flow the pressure level when a gridded ion thruster is operated in a vacuum chamber. Here, two pressure ratios are introduced as expressed in Eqs. (12) and (13), with the pressure within the discharge chamber.

$$\beta = p_b / p_{dc} \tag{12}$$

$$\gamma = p_{dw} / p_{dc} \tag{13}$$

Figure 2 shows the pressure within the discharge chamber of the conventional gridded ion thruster.[5-10] As shown in this figure, the conventional pressure range is from 30 mPa to 100 mPa. The average pressure within the vacuum chamber is 0.1 mPa order for the large vacuum chamber (test facility for the development), or 1 mPa order for the small vacuum chamber (laboratory test facility for the research). Thus, the pressure ratio of to the back pressure to the discharge chamber pressure is from 0.001 to 0.1 for the large vacuum chamber, or over 0.1 for the small vacuum chamber. The discharge chamber pressure in the vacuum chamber operation is expressed in the following equation.

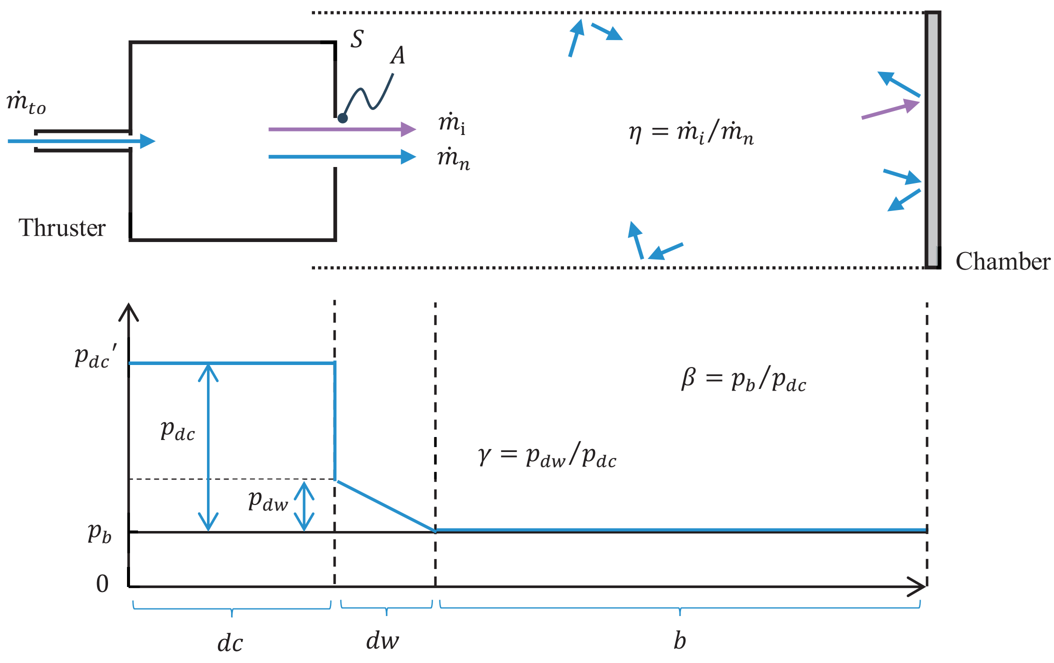

Fig. 1 Schematic of propellant flow and pressure level

$$p_{dc}' = p_{dc} + p_b = (1+\beta)\, p_{dc} \tag{14}$$

Here, the assumption that the ion beam current is proportional to the discharge chamber pressure is adopted for this discussion. Upon considering that the ion beam emitted from the weekly ionized plasma produced in the discharge chamber, the assumption may be appropriated. The thruster performance in the vacuum chamber operation is derived as expressed in the following equations.

$$I_b' = f(\beta) \cdot I_b \approx (1+\beta)\, I_b \propto p_{dc}' \tag{15}$$

$$C_i' = \frac{P_w}{I_b'} = \frac{P_w}{(1+\beta)\, I_b} = \frac{1}{(1+\beta)}\, C_i \tag{16}$$

$$\eta' = (1+\beta)\,\eta \tag{17}$$

The ion thruster durability depends on the charge-exchange current produced in the near downstream region of the thruster. Since the charge-exchange reaction is derived from the collision between the ion and the neutral, the charge-exchange current is proportional to the product of the ion density and the neutral density as expressed in the following equation.

$$I_{CEX} \propto \dot{m}_i \times \dot{m}_n \propto \eta \times (1-\eta)\gamma \tag{18}$$

Derived with these equations, the increase ratio of the charge-exchange current is expressed in the following equation.

$$\frac{I_{CEX}'}{I_{CEX}} = (1+\beta) \cdot \left(1 + \frac{1-\gamma\eta}{1-\eta} \cdot \frac{\beta}{\gamma}\right) \tag{19}$$

The ratio of the pressure in the near downstream to the discharge chamber pressure is derived with the grid aperture ratio of the gridded ion thruster and the conductance of the grid.

$$n_{dc} - n_{dw} = \Delta n = \frac{1}{C_{grd}} \cdot \frac{\dot{m}_n}{M} = \frac{4}{\bar{v}\, A} \cdot \frac{\dot{m}_n}{M} \tag{20}$$

$$n_{dw} = \frac{1}{\bar{v}\,S} \cdot \frac{\dot{m}_n}{M} \tag{21}$$

$$\gamma = \frac{p_{dw}}{p_{dc}} = \frac{n_{dw}}{n_{dc}} = \frac{n_{dw}}{n_{dw} + \Delta n} = \frac{1}{1 + \Delta n / n_{dw}} = \frac{A/S}{4 + A/S} \tag{22}$$

Figure 3 indicates the increase ratio of the charge-exchange current when the aperture ratio is 0.21 that is almost equal to that of the conventional gridded ion thruster. As shown in this figure, especially, the higher the propellant utilization efficiency is, the higher the charge-exchange current is. It becomes clear that the thruster performance and the durability are strongly influenced by the back pressure, in other words, that the performance durability in the vacuum chamber operation is not same as that in the space operation.

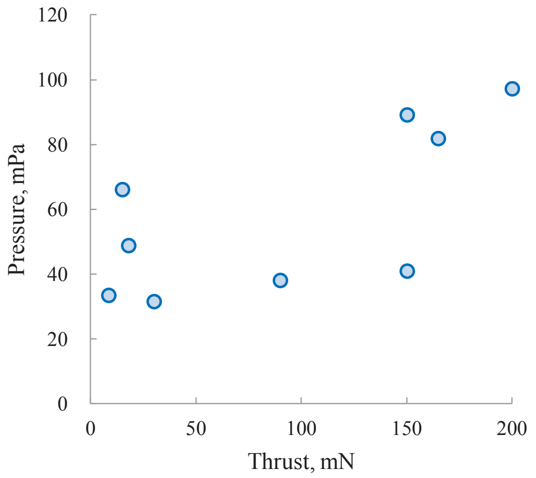

Fig. 2 Discharge chamber pressure of conventional gridded ion thrusters

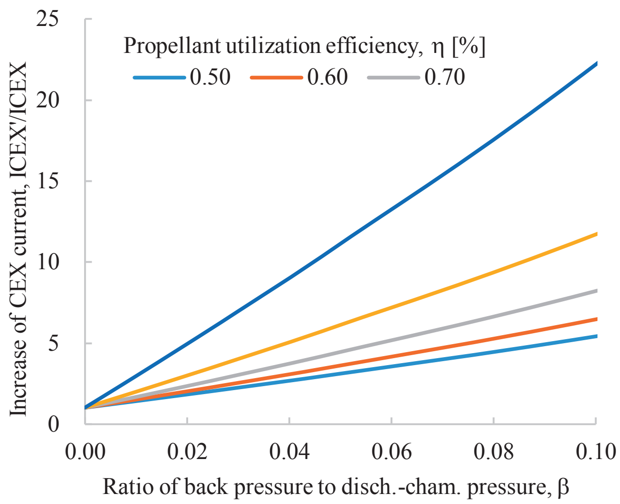

Fig. 3 Influence of back pressure to charge-exchange current

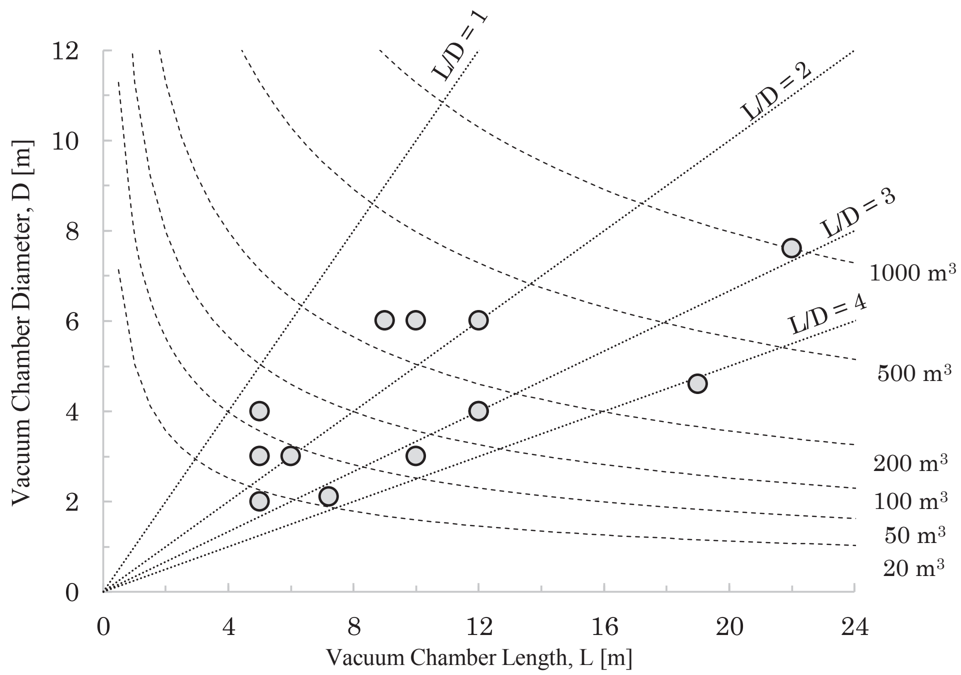

Fig. 4 Vacuum chamber configuration of world EP test facility

III. Numerical Analysis

Numerical analysis is conducted in order to evaluate and discuss influence of the location of the vacuum pumps and the thruster, and to discuss the compensation method for the estimation the thruster performance in space operation from that in the test facility operation.

A. Simulation Model

Figure 4 depicts the configuration of the vacuum chamber operated in the world as the electric propulsion test facility.[11-13] As shown in this figure, it is clear that the aspect ratio of the chamber is from 1 to 4, and that the volume is from 15 m^3 to 1000 m^3. Referring this chamber configurations, in this study, the analytical model vacuum chamber has a cylindrical configuration with the volume of 100 m3, and has an aspect ratio of 1.0, 2.0, or 3.0. The analytical model vacuum pumps has a diameter of 0.80 m, and has an evacuation efficiency of 0.66. Twenty-four pumps are equiangularly placed on the side-wall of the chamber. Any pump is located at 1/4, 2/4, or 3/4 of the chamber length. The temperature on the chamber wall is 300 K. The configuration cases of the vacuum chamber are summarized in Table 1.

Table 2 represents the configuration and performance of the analytical thruster, determined by reference to the SPT-140 hall-effect ion thruster.[14] The thruster is located on the center axis of the vacuum chamber. The distance between the thruster and the upstream surface of the chamber is 0.5 m or 1.0 m.

In this study, the DSMC method code developed in our previous study is used for this numerical analysis.[15-17] This DSMC, direct simulation Monte Carlo, is a numerical method modeling rarefied particle flows. In this simulation, any analytical particle is irregularly reflected on the chamber wall with the thermal velocity. The thermal velocity is determined to satisfy the Boltzmann distribution depending on the temperature of the chamber wall surface.

Table 1 Vacuum chamber configuration

Type	shape			number of pumps		
	D [m]	L [m]	L/D	at 1/4 L	at 2/4 L	at 3/4 L
D50L050P040812	5.0	5.0	1.0	4	8	12
D50L050P041208	5.0	5.0	1.0	4	12	8
D50L050P080412	5.0	5.0	1.0	8	4	12
D50L050P081204	5.0	5.0	1.0	8	12	4
D50L050P120408	5.0	5.0	1.0	12	4	8
D50L050P120804	5.0	5.0	1.0	12	8	4
D50L050P080808	5.0	5.0	1.0	8	8	8
D40L080P040812	4.0	8.0	2.0	4	8	12
D40L080P041208	4.0	8.0	2.0	4	12	8
D40L080P080412	4.0	8.0	2.0	8	4	12
D40L080P081204	4.0	8.0	2.0	8	12	4
D40L080P120408	4.0	8.0	2.0	12	4	8
D40L080P120804	4.0	8.0	2.0	12	8	4
D40L080P080808	4.0	8.0	2.0	8	8	8
D35L105P040812	3.5	10.5	3.0	4	8	12
D35L105P041208	3.5	10.5	3.0	4	12	8
D35L105P080412	3.5	10.5	3.0	8	4	12
D35L105P081204	3.5	10.5	3.0	8	12	4
D35L105P120408	3.5	10.5	3.0	12	4	8
D35L105P120804	3.5	10.5	3.0	12	8	4
D35L105P080808	3.5	10.5	3.0	8	8	8

Table 2 Thruster configuration

dimeter	0.20 m
length	0.20 m
main flow rate	160 sccm
neut. flow rate	20 sccm
beam div. angle	40 deg.
propellant util. eff.	75%
acceleration potential	300 V
thrust	300 mN

B. Simulation Results and Discussion

Figure 5 shows the pressure distribution within the analytical vacuum chamber. As shown in this figure, the pressure distribution is non-homogeneous, although the distribution is almost symmetric with respect to the center axis of the analytical chamber.

Figure 6a indicates the average pressure and the downstream pressure against the aspect ratio of the analytical chamber. As shown in this figure, both the average pressure and the downstream pressure is lower as the aspect ratio of the analytical chamber approaches to 1.0. This supports the theoretical analysis as mentioned in the section II-A.

Figure 6b indicates the average pressure and the downstream pressure with respect to the average distance between the analytical thruster and the vacuum pumps. As shown in this figure, the pressure is almost proportional to the average distance.

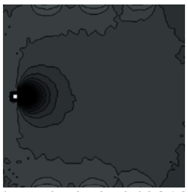

(a) D50L050P040812

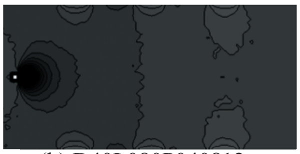

(b) D40L080P040812

(c) D35L105P040812

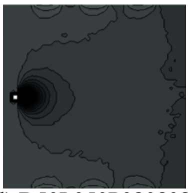

(d) D50L050P080808

(e) D40L080P080808

(f) D35L105P080808

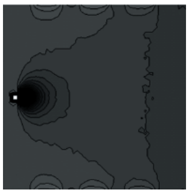

(g) D50L050P120804

(h) D40L080P120804

(i) D35L105P120804

from (a) to (i) : thruster location at 0.5 m spaced from upstream surface of vacuum chamber

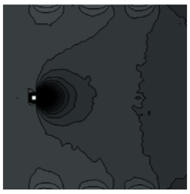

(j) D50L050P040812

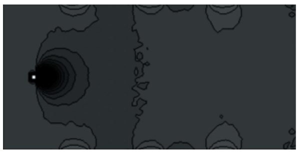

(k) D40L080P040812

(l) D35L105P040812

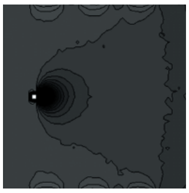

(m) D50L050P080808

(n) D40L080P080808

(o) D35L105P080808

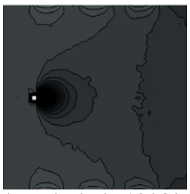

(p) D50L050P120804

(q) D40L080P120804

(r) D35L105P120804

from (j) to (r) : thruster location at 1.0 m spaced from upstream surface of vacuum chamber

Fig. 5 Pressure distribution within vacuum chamber with 24 vacuum pumps and a thruster

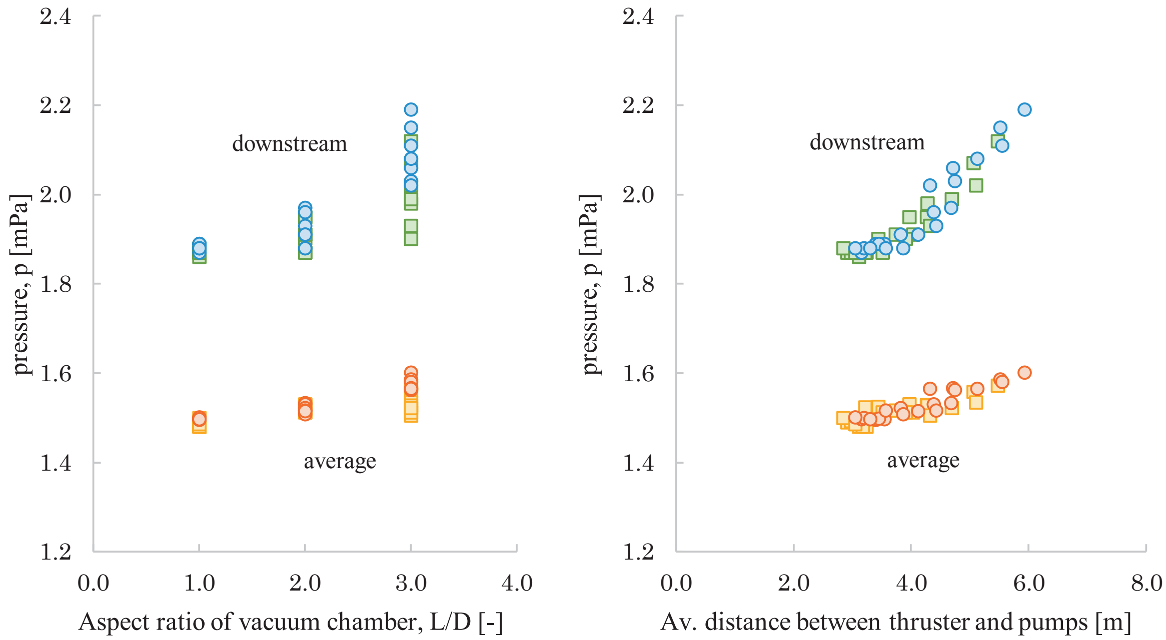

(a) Pressure vs. aspect ratio **(b) Pressure vs. average distance**

Figure 6 Average pressure and downstream pressure in analytical vacuum chamber

C. Discussion on Vacuum Chamber Design

Judging from these results and discussion, the following design-approaches are proposed for the appropriate vacuum chamber as the electric propulsion test facility:

(1) Many vacuum pumps installed on the chamber, as much as possible
(2) Aspect ratio of the vacuum chamber approaches 1.0, as less as possible
(3) Average distance between the thruster and the pumps is lower.

These are because the back pressure, the average pressure within the chamber strongly affects the performance and the durability.

Although the application of approaches (1) and (2) to the existing test facility is very difficult, the approach (3) may be applicable with relatively little effort: by the modification of the thruster location.

D. Discussion on Thruster Performance Prediction

In general, the pressure of the vacuum chamber is measured with a vacuum gage. As discussed in the above, however, the measured pressure is not the same as the average pressure within the vacuum chamber. Thus, in this study, the following approaches are proposed for the thruster performance prediction with the experimental measured performance in the test facility operation:

(1) First of all, numerical simulation of the pressure distribution with in the chamber is conducted.
(2) Second, the difference between the pressure on the gauge location and the average pressure is determined.
(3) Third, the thruster performance is measured in the original test facility operation.
(4) Fourth, the thruster performance is measured in higher pressure operation in the same facility, with an auxiliary propellant supply through the chamber wall, not through the thruster.
(5) Fifth, the relation between the back pressure and the performance, for example, as expressed in Eq. (15).
(6) Finally, the thruster performance and durability are predicted, derived from the inverse-calculation with the equations mentioned in the section II.

E. Future Works

In this study, the influence and performance in the relatively-large test facility operation are discussed. However, many laboratory has not the large vacuum chamber, but several relatively-small vacuum chamber for the researches. In general, the small chamber has a vacuum pump. This means that the pressure distribution is more significant inhomogeneous. Therefore, more careful discussion is necessary.

IV. Concluding Remarks

Through the theoretical analysis and numerical simulation, the following remarks were obtained.

(1) The pressure distribution within the vacuum chamber is non-homogeneous.
(2) The aspect ratio of the vacuum chamber influences the average pressure: the back pressure.
(3) The average distance between the thruster and the pumps influences the back pressure.
(4) The back pressure significantly affects the thruster performance and the durability.
(5) A thruster performance prediction method is proposed in this study.
(6) For the relatively-small vacuum chamber, more careful discussion is necessary.

Acknowledgments

The authors thank Lt. Kenichi Narisawa of Japan Ground Self Defense Force for his help in numerical simulation.

References

[1] David Byers, John W. Dankanich. "A Review of Facility Effects on Hall Effect Thrusters" *31th International Electric Propulsion Conference*, IEPC-2009-076, USA, 2009.

[2] Richard R. Hofer. Peter Y. Peterson. Alec D. Gallimore. "Characterizing Vacuum Facility Backpressure Effects on the Performance of a Hall Thruster" *27th International Electric Propulsion Conference*, IEPC-2001-045, USA, 2001.

[3] Iain D. Boyd, Chunpei Cai, Mitchell L. R. Walker and Alec D. Gallimore. "Computation of Neutral Gas Flow from a Hall Thruster into a Vacuum Chamber" Rarefled Gas Dynamics: *23rd International Symposium*, USA, 2003.

[4] Mitchell L. R. Walker and Alec D. Gallimore. "Neutral density map of Hall thruster plume expansion in a vacuum chamber" 2005 American Institute of Physics, USA, 2005.

[5] Nishiyama, K. and Kuninaka, H., "Discussion on Performance History and Operations of Hayabusa Ion Engines," *Transactions of JSASS Space Technology Japan*, Vol. 10, Pb.Tb_1-Tb_8, 2012.

[6] Nishiyama, K., Hosoda, S., Ueno, K. and Kuninaka, H., "The Ion Engine System for Hayabusa2" *32th International Electric Propulsion Conference*, IEPC-2011-309, Germany, 2011.

[7] Kuriki, K. and Arakawa, Y., *Introduction to Electric Propulsion*, University of Tokyo Press,, Tokyo, 2003, pp115,234-236 (in Japanese).

[8] Goebel, D., Polk, J., Sandler, I., Mikellides, I., Brophy, J., Tighe, W. and Chien. K., "Evaluation of 25-cm XIPS© Thruster Life for Deep Space Mission Application," *31th International Electric Propulsion Conference*, IEPC-2009-152, USA, 2009.

[9] Nakayama, Y. and Narisawa, K., "Neutral Density Measurement of Ion Thruster with Differential Pressure Gauge," *Transactions of JSASS Space Technology Japan*, Vol. 12, p.Pb_73-Pb_78, 2014.

[10] Nakayama, Y. and Narisawa, K., "Neutral Pressure Measurement in an Ion Thruster Discharge Chamber" *33th International Electric Propulsion Conference*, IEPC-2013-106, USA, 2013.

[11] Arakawa, Y., Kuninaka, H., Nakayama, Y. and Nishiyama, K., *Ion Engine for Powered Flight in Space*, Corona, Tokyo, 2006 (in Japanese).

[12] Gonzalez, J. and Saccoccia, G. "ESA Electric Propulsion Activities", *32th International Electric Propulsion Conference*, IEPC-2011-329, Germany, 2011.

[13] M. Saverdi, M. Signori, L. Milaneschi, U. Cesari and L. Biagioni, "The IV10 Space Simulator for High Power Electric Propulsion Testing: performance Improvements and Operation Status" 30*th International Electric Propulsion Conference*, IEPC-2007-321, Italy, 2007.

[14] David Manzella. "Performance Evaluation of the SPT-140," NASA TM-206301, 1997

[15] Boyd, I. D. "Numerical modeling of spacecraft electric propulsion thrusters," *Progress in Aerospace Sciences*, Vol. 41, No. 8., 2005, pp.669-687.

[16] Mahalingam, S., Choi, Y., Loverich, J., Stoltz, P. H., Bias, B., and Menart, J. A. "Fully Coupled Electric Field/PIC-MCC Simulation Results of the Plasma in the Discharge Chamber of an Ion Engine," *47th AIAA Joint Propulsion Conference*, AIAA-2011-6071, USA, 2011.

[17] Miyasaka, T., Kobayashi, T., and Asato, K. "Characteristics of ions impacting grid surfaces in an ion engine," *Vacuum*, Vol. 85, No. 5, 2010, pp.585-590.